A Novel Single Phase Cascaded Multilevel Inverter for Hybrid Renewable Energy Sources

Kaliamoorthy M, *Member, IEEE,* Rajasekaran V, *Member, IEEE,* PraveenRaj G, *Member, IEEE,*

***Abstract*—This paper presents a novel single phase cascaded multilevel inverter for renewable energy applications. The proposed inverter consists of two H Bridge inverter connected in cascade. The top H Bridge inverter is a conventional H bridge inverter and is capable of developing three level output whereas the bottom H bridge inverter is a novel inverter which is capable of developing multilevel output. The proposed inverter is driven from a novel hybrid modulation technique, which eliminates the problem of capacitor voltage balancing issues. The proposed novel hybrid modulation technique switches the top inverter switches at high frequency and the bottom inverter switches at low frequency. The proposed inverter can be fed from any renewable energy source. In this paper, the top inverter is fed from PV arrays where as the bottom inverter is fed from wind turbine. The proposed inverter has many advantages such as; it has minimum number of power electronic devices, minimum conduction and switching losses, improved efficiency and minimum voltage stress on the devices. The proposed inverter fed from renewable energy sources is simulated in MATLAB/SIMULINK environment. To validate the simulation results a laboratory prototype is also built. The entire hardware setup is controlled by using FPGA-SPATRAN 3A DSP board.**

Keywords: Multilevel inverter, Hybrid modulation technique, Capacitor voltage balancing, PV array and Wind Turbine.

I. Introduction

MICROGRID research is gaining more and more importance due to the need of economic usage of electric power. Nowadays, fossil fuel is the main energy supplier of the world wide economy, but it is a major cause of ecological problems (such as global warming, air pollution etc.). The need of producing more energy combined with the interest in green energy technologies results in an increased development of power distribution systems using renewable energy sources (RES) such as wind energy, solar, hydro, biomass, wave energy, tidal power and geo thermal energy [1]. Further stress on the present electrical power system is also increasing, due to the increase in power demand, limitation on power delivery capability of the grid, complications in building new transmission - distribution lines, and leading to blackouts [1]. Developments of power electronic converters along with its high-performance controllers make it possible to integrate different types of renewable energy sources to the microgrid.

Different converter topologies as well as control methods to integrate renewable energies, i.e., wind power and solar power, etc., in power grids are surveyed in details in [2]-[10]. In the cited papers, it can be seen that extensive research is undertaken to connect renewable energy sources to three-phase grids using three-phase pulse-width-modulation (PWM) inverters. In case of medium power microgrid application, single-phase inverters are gaining popularity [11]-[25]. The existing literature show that on one hand, the single-phase inverter is directly connected (through an interfacing choke coil) to the point of common coupling (PCC) [11] to facilitate power flow to PCC. On the other hand, the grid (microgrid) and the loads are also connected to the PCC. In a typical residential application, the renewable energy is used to reduce the load power demand from the microgrid.

The energy from the renewable/natural sources tends to vary throughout the day and hence optimizing the energy capture is a necessity.For wind turbines (WT) and PV arrays, the output power is determined by the wind speed and irradiation. Hence, the control of these systems needs to behave appropriately according to the variation of these parameters. For example, the turbine speed for wind needs to be adjusted for different wind speeds such that the generated power available is optimized and the system runs at Maximum Power Point (MPP).Similarly,the output DC voltage and current of the PV array systems need to be adjusted in order to run them at MPP.Numerous types of converters have been used to provide grid connected renewable energy systems. In PV applications, DC-DC converters are utilized to regulate the variable and low quality output voltage of PV panels. A DC- AC converter is used to generate desired voltage and frequency for the grid connection. Similarly, AC-DC-AC converter is essential for the WECS as wind energy is variable.

Due to the rising demand for medium and high power applications, multilevel inverters (MLI) have been attracting and growing consideration in variable speed WT and PV systems recently [3],[4]. Multilevel converters enable the output voltage to increase without increasing the voltage rating of the switching devices, so that they offer the direct connection of renewable energy systems to the grid voltage without using the expensive and bulky transformers. Various topologies of multilevel inverter have been investigated in the literature. The most common types among them are the diode clamped [5], the flying capacitor [6] [7], the Cascaded H-bridge multilevel inverters (CHBMLI) [8] [9], modified H-bridge multilevel inverters [10] and the full bridge with cascaded transformers [11].

Among the various types of multilevel inverter, cascaded type is more popular especially in particular for grid connected

M.Kaliamoorthy is with the Department of Electrical and Electronics Engineering, PSNA College of Engineering and Technology, Dindigul, Tamilnadu, 624622 India e-mail:kaliasgoldmedal@gmail.com (see http://www.kaliasgoldmedal.yolasite.com).

Dr.V.Rajasekaran is Professor and Head Dept of EEE,PSNACET.Dindigul.

G.Praveenraj is PG Scholar Dept of EEE,PSNACET.Dindigul.

978-1-4779-6438-3/15/$31.00

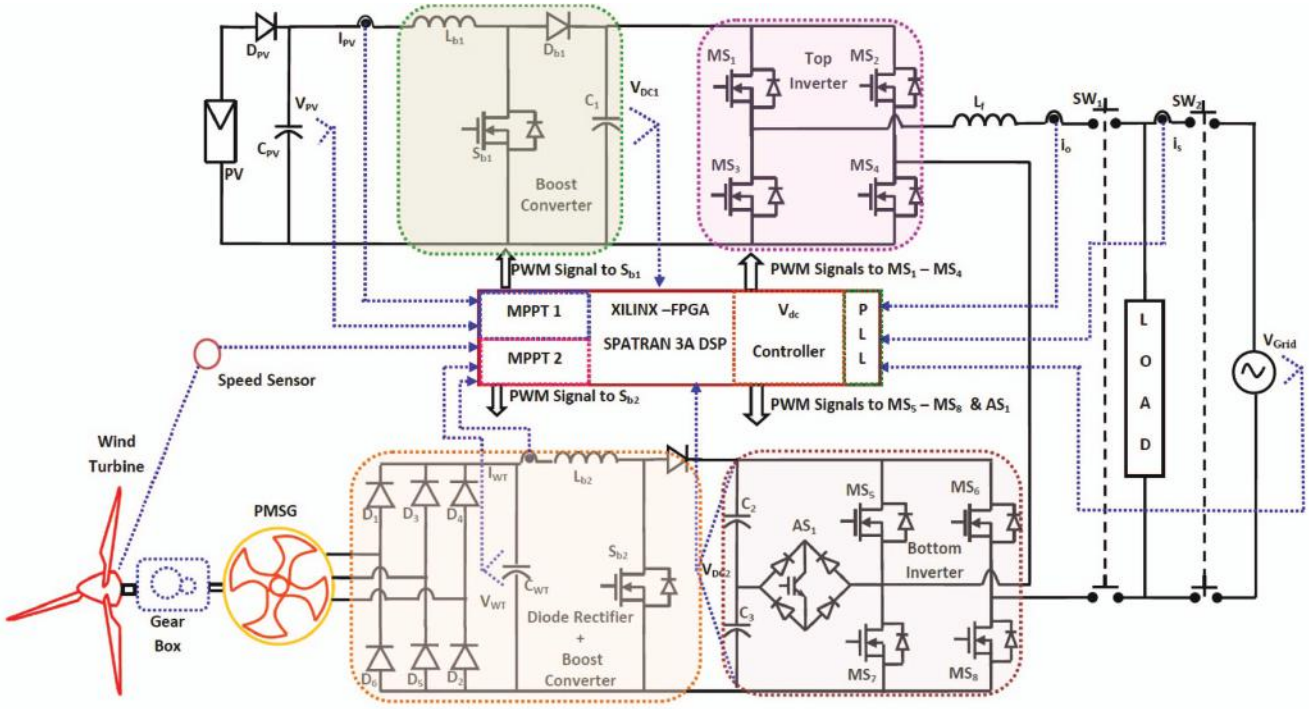

Fig. 1. Proposed Cascaded H Bridge Multilevel Inverter.

renewable energy applications due to the following reasons,

1. Individual H bridge can be connected to a separate renewable energy sources such as PV modules, Wind Turbines, Fuel Cell stacks etc.

2. Step up transformers are eliminated since the output voltage level required for grid power injection can be achieved by DC-DC boost converters and the cascaded connection of H bridge outputs.

3. The CHBMLI has very less total harmonic distortion (THD) when compared to three-level based inverters, which in turn reduces the output filter size for the compliance of grid harmonic standards [12].

4. Since this topology allows the connection of independent renewable energy sources each dc link voltages can be independently controlled, the maximum power extraction of a reduced number of PV modules can be accomplished with the help of Maximum Power Point Tracking (MPPT) algorithms [14].

This paper proposes a novel single phase grid connected multilevel inverter fed from PV arrays and wind turbine coupled permanent magnet synchronous generator (PMSG). The proposed inverter is switched by hybrid modulation technique. In order to track the MPP of the PV array and the wind turbine a novel sliding mode control strategy is used, which is more accurate and fast in tracking the MPP for varying environmental conditions.

II. System Configuration

The proposed single phase eleven level grid connected MLI is an enhanced version of the inverter developed in [9]. It consists of two inverters connected in cascade (namely upper and lower inverters). The upper inverter is a conventional H bridge inverter, where as the lower inverter is the one established in [9]. Fig 1 shows the circuit configuration of the proposed multilevel inverter. This proposed inverter configuration has lot of advantages such as less number of power electronic devices, power diodes, capacitors and isolated DC sources when compared with other configurations and is best suited for renewable energy applications.

The upper inverter is fed from a PV module through a DC-DC boost converter and the lower inverter is fed from a wind turbine driven PMSG through an uncontrolled rectifier and a DC-DC boost converter. The DC-DC boost converter in the upper inverter is used to track the MPP of the PV module. The uncontrolled rectifier in the lower inverter converts the AC voltage generated from the PMSG to a DC voltage. The DC-DC boost converter in the lower inverter is used to track the MPP of the wind turbine and to convert the rectified DC voltage to a high voltage DC. High dc bus voltages are essential to make sure that power flows from the PV module and the wind turbine to the grid. A filtering inductance Lf is used to filter the current injected into the grid. Switches SW1 and SW2 are used to disconnect the PV power generation system and wind energy conversion system from the grid during islanding operation. The load is placed between switches SW1 and SW2. By switching the inverter properly, it can produce eleven output voltage levels from the DC supplies.

A. Operation of the proposed multilevel inverter

The proposed multilevel inverter configuration is of asymmetrical type. The magnitude of each DC link capacitor in the lower inverter is two times the upper H bridge capacitor.(i.e

TABLE I
SWITCHING STATES OF PROPOSED INVERTER

Upper Inverter Switches (High Frequency Switches)				Lower Inverter Switches (Low Frequency Switches)					Derived Output Voltage $V_{dc1} = V_{dc2} = 2V_{dc0}$			
MS_1	MS_2	MS_3	MS_4	MS_5	MS_6	MS_7	MS_8	AS_1	V_{up}	V_{low}	V_{total}	Mode
ON	OFF	OFF	ON	ON	OFF	OFF	ON	OFF	$0 \leftrightarrow V_{dc0}$	$4V_{dc0}$	$4V_{dc0} \leftrightarrow 5V_{dc0}$	I
OFF	ON	ON	OFF	ON	OFF	OFF	ON	OFF	$-V_{dc0} \leftrightarrow 0$	$4V_{dc0}$	$3V_{dc0} \leftrightarrow 4V_{dc0}$	II
ON	OFF	OFF	ON	OFF	OFF	OFF	ON	ON	$0 \leftrightarrow V_{dc0}$	$2V_{dc0}$	$2V_{dc0} \leftrightarrow 3V_{dc0}$	III
OFF	ON	ON	OFF	OFF	OFF	OFF	ON	ON	$-V_{dc0} \leftrightarrow 0$	$2V_{dc0}$	$V_{dc0} \leftrightarrow 2V_{dc0}$	IV
ON	OFF	OFF	ON	ON	ON	OFF	OFF	OFF	$0 \leftrightarrow V_{dc0}$	0	$0 \leftrightarrow V_{dc0}$	V
OFF	ON	ON	OFF	OFF	OFF	ON	ON	OFF	$0 \leftrightarrow -V_{dc0}$	0	$0 \leftrightarrow -V_{dc0}$	VI
ON	OFF	OFF	ON	OFF	ON	OFF	OFF	ON	$V_{dc0} \leftrightarrow 0$	$-2V_{dc0}$	$-V_{dc0} \leftrightarrow -2V_{dc0}$	VII
OFF	ON	ON	OFF	OFF	ON	OFF	OFF	ON	$0 \leftrightarrow -V_{dc0}$	$-2V_{dc0}$	$-2V_{dc0} \leftrightarrow -3V_{dc0}$	VIII
ON	OFF	OFF	ON	OFF	ON	ON	OFF	OFF	$V_{dc0} \leftrightarrow 0$	$-4V_{dc0}$	$-3V_{dc0} \leftrightarrow -4V_{dc0}$	IX
OFF	ON	ON	OFF	OFF	ON	ON	OFF	OFF	$0 \leftrightarrow -V_{dc0}$	$-4V_{dc0}$	$-4V_{dc0} \leftrightarrow -5V_{dc0}$	X

$V_{dc2} = V_{dc3} = 2V_{dc1}$). Hence, the DC link voltage of the lower H bridge is four times the DC link voltage of the upper H bridge.Thus 90 of the power fed to the load is from the lower inverter and the upper inverter supplies only 10. The upper H bridge inverter is a conventional inverter which generates three level output $(+V_{dc1}, 0, -V_{dc1})$. The lower H bridge inverter is capable of generating five level output ($+2V_{dc1}, V_{dc1}, 0, -V_{dc1}, -2V_{dc1}$). The lower H bridge inverter operation can be divided into five switching states, as shown in Fig. $2(a) - (f)$.

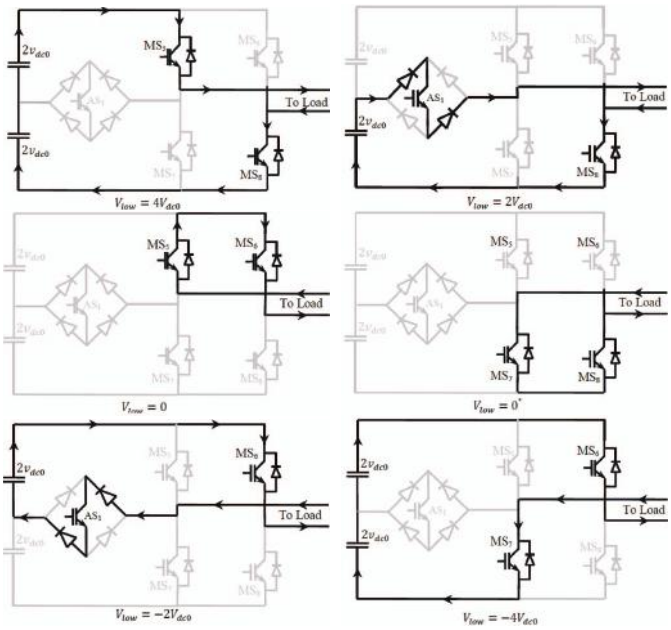

Fig. 2. Operation of Lower Inverter.

TABLE II
SWITCHING STATES OF LOWER H BRIDGE INVERTER

V_{low}	MS_5	MS_6	MS_7	MS_8	AS_1	Reference
$4V_{dc}$	ON	OFF	OFF	ON	OFF	Fig 2(a)
$2V_{dc}$	OFF	OFF	OFF	ON	ON	Fig 2(b)
0	ON	ON	OFF	OFF	OFF	Fig 2(c)
0	OFF	OFF	ON	ON	OFF	Fig 2(d)
$-2V_{dc}$	OFF	ON	OFF	OFF	ON	Fig 2(e)
$-4V_{dc}$	OFF	ON	ON	OFF	OFF	Fig 2(f)

Fig. 2(a) and (f) are switching sequences of the lower inverter in the conventional mode. Fig. 2(b) and (e) show the additional switching sequence of the lower H bridge. The combined switching combinations of the upper and lower H bridge inverter to develop eleven levels at the load terminals are given in Table 1.

B. Hybrid PWM switching strategy

To minimize the switching losses in the proposed multilevel inverter, hybrid PWM (Pulse Width Modulation) switching strategy is used [15],[34]. Since most of the power fed to the load is from the lower inverter, the switches of the lower H bridge inverter are switched at fundamental frequency (i.e. at 50Hz). Whereas, the upper H bridge inverter switches are switched at high frequency (i.e. at 10 KHz). Fig 3 shows the modulation strategy of the proposed inverter. The signals R_{01} and R_{02} shown in fig 3 are responsible for generation of PWM pulses for the upper inverter. Signal R_{01} is compared with the high frequency carrier to generate PWM for MS_1 and MS_4 similarly R_{02} generates PWM for MS_2 and MS_3. Since the lower inverter switches at low frequency, the switching signal generation of lower inverter switches can be determined easily by simple arithmetic and logical computations. The switching signals for the lower inverter are also shown in fig 3.

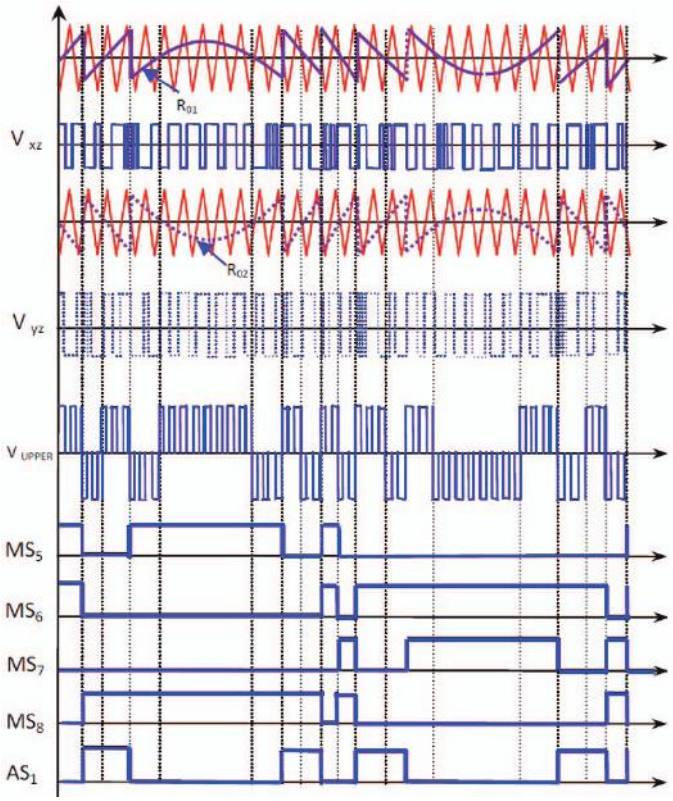

Fig. 3. Modulation Strategy of the Proposed Inverter.

The total reference waveform of the inverter is generated as shown in Fig. 4 (a) and defined in (1).

$$U_{ref} = sin(\omega t). \tag{1}$$

The reference waveform for the upper inverter is generated by using the following expressions:

$$Z_1 = \begin{cases} 1 & if U_{ref} > 0 \\ 0 & if U_{ref} < 0 \end{cases} \tag{2}$$

$$V_{Lower,expected} = \left(round\left(\frac{|U_{ref}|}{0.4}\right) * 0.4 * Z_1 \right) + \left(round\left(\frac{|U_{ref}|}{-0.4}\right) * 0.4 * \bar{Z}_1 \right) \tag{3}$$

$$R_{01} = 5 * (U_{ref} - V_{Lower,expected}) \tag{4a}$$

$$R_{02} = 1 - [5 * (U_{ref} - V_{Lower,expected})] \tag{4b}$$

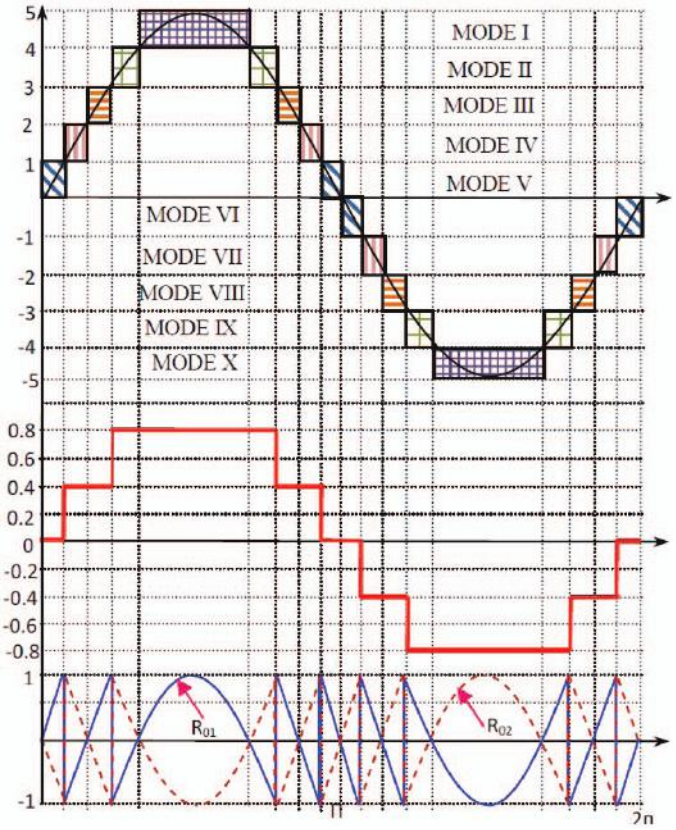

Fig. 4. Reference Waveform Generation for an 11 level Inverter (Upper Bridge).

The waveform representation of the equations (1), (3) and (4) are shown in fig 4. The reference waveform for the lower inverter is given by,

$$V_{Lower,ref} = round\left(\frac{|U_{ref}|}{0.4}\right) \tag{5}$$

The next step is to divide the lower inverter reference signal (5) into two signals (i.e. $R_{01} and R_{02}$) and they are given as,

$$R_1 = \begin{cases} 1 & : if V_{Lower,ref} > 1 \\ 0 & : if V_{Lower,ref} < 0 \end{cases} \tag{6a}$$

$$R_2 = \begin{cases} 1 & : if V_{Lower,ref} > 2 \\ 0 & : if V_{Lower,ref} < 0 \end{cases} \tag{6b}$$

The H bridge switches of the lower inverter are switches as per the equations given below,

$$MS_5(t) = \left[\left(\bar{R}_1\right) + (R_2)\right] * (Z_1) \tag{7}$$

$$MS_6(t) = \left[(R_1) * \left(\bar{Z}_1\right)\right] + \left[\left(\bar{R}_1\right) * (Z_1)\right] \tag{8}$$

$$MS_7(t) = \left[\left(\bar{R}_1\right) + (R_2)\right] * \left(\bar{Z}_1\right) \tag{9}$$

$$MS_8(t) = \left[(R_1) * (Z_1)\right] + \left[\left(\bar{R}_1\right) * \left(\bar{Z}_1\right)\right] \tag{10}$$

Where + denotes logical OR operation and * denotes multiplication of signals. The switching patterns of auxiliary switch AS1 is given by

$$AS_1(t) = \left((R_1 \oplus R_2) * \bar{Z}_1\right) \tag{11}$$

where $\oplus$ denotes XOR operation.

III. Sliding Mode Control Based MPPT for PV module and Wind Turbine

At given environmental conditions, PV module and WT supply maximum power at a particular operating pointthe maximum power point (MPP). In order to make use of the nature power effectively, it is necessary to operate PV module and WT at their MPP [16]-[20]. However, the locus of MPP varies over a wide range, depending on the climatic conditions [21], [22]. For example MPP of PV module depends on its temperature and insolation intensity and MPP of WT depends upon the wind velocity, which varies throughout the day. Many authors have proposed different solutions [23]-[26]. Some of them are better during steady state [23], [24], while others show superior performance transitions [25][26]. The perturb and observeand the Hill-Climbing algorithms are probably those most widely used. The operating principle is almost similar in both the algorithms, in case of the PV module the voltage and current of the PV generator are sensed and the power is calculated where as in the case of WT, speed and torque are sensed and the power is calculated. Then, the MPP is sought iteratively.

These algorithms involve a trade off in selecting the increment value by which the control factor, such as reference voltage, current or duty cycle is tuned. When small values are chosen, the losses are decreased in steady state because of small perturbations around the MPP but gives poor dynamic performance. On the other hand large values improve the dynamic behavior but gives large steady state error [25][26]. The presented sliding mode control based MPPT improves the dynamic performance and reduces the steady state error. Fig 5(a) shows the VI characteristics of TATA BP solar PV module (TP 180) for various insolation conditions. Once the VI characteristics are simulated for various irradiance levels, MPP data can be easily identified from the simulation data array. All the MPP for various irradiance levels are joined together to form a curve by using curve fitting tool of MATLAB/SIMULINK. The equation of the curve is also given in figure 5(a). The electrical parameters at standard testing conditions (STC) are given in table 2.

The system used for MPPT is shown in fig 1. Assuming a large output capacitor ($C_1, C_2 and C_2$ in fig 1) and the DC-DC boost converter output voltage is assumed to be almost constant. Thus, the PV module voltage and current form all the converters state variables, which give the switching surface as given by (12).

TABLE III
PARAMETERS OF PV MODULE UNDER STC (STANDARD TESTING CONDITIONS 1000 W/m^2, 25^0C)

Parameter	Value
Power Output P_{MAX} (W)	180
Voltage at P_{MAX}, V_{MAX} (V)	35
Current at P_{MAX}, I_{MAX} (A)	5.03
Open Circuit Voltage V_{oc} (V)	43.6
Short Circuit Current I_{sc} (V)	5.48

TABLE IV
PARAMETERS OF WT AND PMSG

Wind Turbine Parameters		PMSG Parameters	
Rated Power (KW)	2	Rated Power (KW)	3
Rated wind speed (m/s)	10	Stator resistance (Ohms)	1.5
Radius (m)	1.525	Stator inductance (mH)	0.01
Gear Ratio	5	Pole Pairs	2
Air density m3/Kg	1.08	Flux (Wb)	0.2194
Height (m)	5	Moment of Inertia (kg m)	2

$$S\left(v,i\right) = a.i - \left(b.v^3 + c.v^2 + d.v + e\right) = 0 \qquad (12)$$

where $(a, b, c, d, e) > 0$, $S < 0 \Rightarrow$ ON state, $S > 0 \Rightarrow$ OFF state

Where v and i are PV module voltage and inductor current, and a, b, c, d and e define the switching surface. a, b, c and d set the slope in the PV module v-i plane and e sets the offset. When S ¡ 0 (ON State), S_{b1} switch in fig 1 is turned ON and the inductor gets charged. The current i through the inductor increases, and S (v, i) increases. When S ¿ 0 S_{b1} is turned OFF and the energy stored in the inductor discharges through the load. Thus the current i through the inductor decreases as a result S (v, i) also decreases. Thus, S (v, i) is kept in a switching band around S =0. Similarly fig 5 (b) shows the speed Vs power characteristics of WT for various wind speeds. The details of the wind turbine and PMSG used in this study are given in table 3. The same procedure is repeated to track the MPP of wind turbine. The sliding surface for WT is as given by (13).

$$S_{wt}\left(v,i\right) = a.p - \left(b.v^2 + c.v + d\right) = 0 \qquad (13)$$

where $(a, b, c, d) > 0$, $S_{wt} < 0 \Rightarrow$ ON state, $S_{wt} > 0 \Rightarrow$ OFF state

Where p and n are the WT power and speed. When $S_{wt}(p, n) < 0$ (ON state), S_{b2} in fig 1 is turned ON and the inductor charges.The current i through the inductor increase, which in turn increases the sliding surface $S_{wt}(p, n)$. When $S_{wt}(p, n) > 0$ S_{b2} is turned OFF and the energy stored in the inductor discharges to the load. Thus the current i through the inductor decreases as a result $S_{wt}(p, n)$ also decreases. Thus, $S_{wt}(p, n)$ is kept in a switching band around $S_{wt}(p, n) = 0$. Fig 6 shows the performance of the proposed sliding mode controlled MPPT algorithm for PV modules (Fig 6(a)) and WT (Fig 6(b)). It is clear from the figure 6 that steady state and dynamic performance of the MPPT algorithms is good and it perfectly match with that of the actual MPP (refer data points in Fig 5).

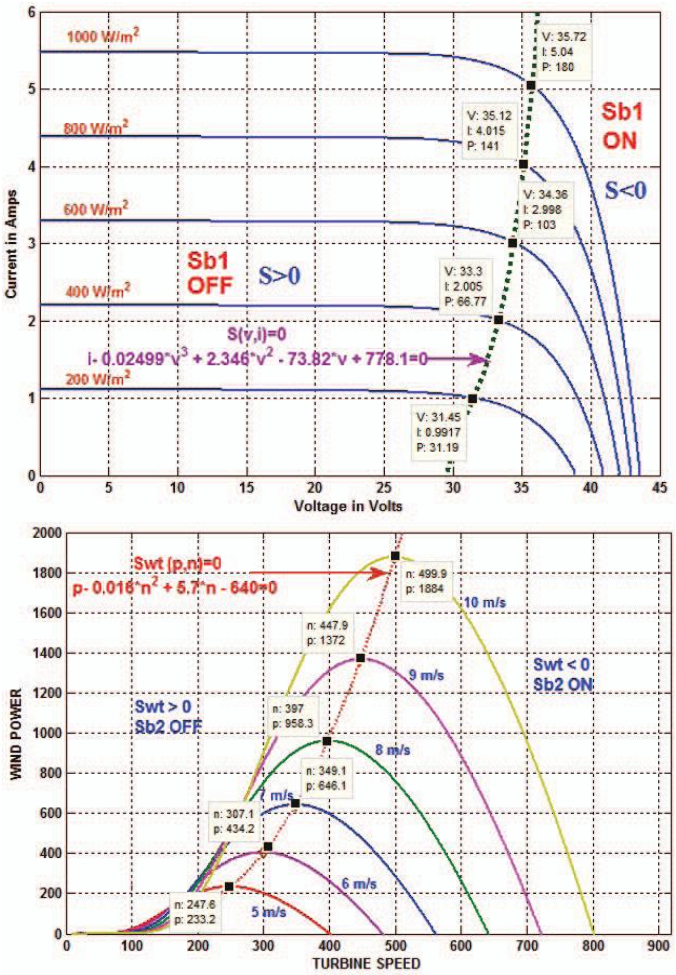

Fig. 5. (a) VI characteristics of PV module under different irradiance and the optimal switching surface (green), S (v, i) =0.
(b)Wind Turbine Speed Vs Power Characteristics for various wind speeds and the optimum switching surface (red) $S_{wt}(p, n) = 0$.

IV. CONTROL OF GRID CONNECTED MULTILEVEL INVERTER

This section presents a method for controlling a multilevel inverter which interfaces PV sources and WT to the grid. The proposed system, as show in Fig. 7, is proficient of maintaining system performance despite of environmental conditions. This system topology is composed of two circuits which have a dc-dc converter at the input, a dc-link capacitor, and an H bridge at the output. Both these circuits will be referred to as a sub-inverter. Both sub-inverters are connected in series and then interfaced to the grid via an inductive output filter. Energy balance is managed by a single master controller and two local sub-inverter controllers.

A master controller is used to manage energy flow between the aggregate system of sub-inverters and the grid-utility. In particular, the main functions of the master controller are to regulate the output current, io, and to manage the total voltage across the dc-link capacitors. The master controller generates a master modulation signal, M_{SYS}, which is then fed to the individual sub-inverter controllers. Each local controller then scales M_{SYS} to create a unique modulation signal, M_1 and

M_2 such that the local dc-link capacitor voltage is regulated. In addition, both PV source and WT is interfaced to a dc-dc converter which performs MPPT. From inspection of Fig.7, is apparent that the MPPT controllers are decoupled from the rest of the control system. With the proposed controller, the task of capacitor voltage balancing is decomposed into two separate problems. Namely, the master controller regulates the aggregate sum of the capacitor voltages and the local controllers manage their respective dc-link voltage.

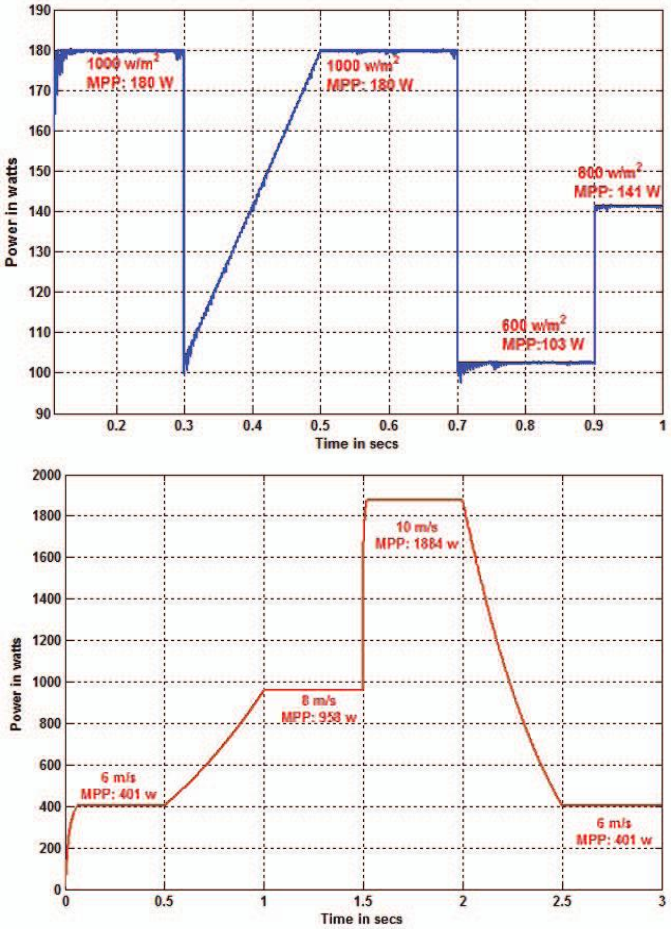

Fig. 6. Performance of sliding mode control based MPPT for sudden variations in environmental conditions (a) PV module (b) Wind Turbine.

A. Master Controller

The master controller, as illustrated in Fig. 8, has two purposes: i) regulate the sum of the dc-link voltages to a prescribed value, and ii) deliver a sinusoidal output current to the grid. The first objective can be recast in terms of energy balance. Since the dc-link capacitors are energy storage devices, their voltages can be maintained by ensuring that the energy generated by the PV and WT (minus losses) is delivered to the grid. The current control stage can be designed using conventional current control methods. Each of the two master control sections is described below. If the total power conversion loss is p_{loss}, RMS output current is I_{rms} and peak output current is i_{pk}, then the energy conversion can be written as,

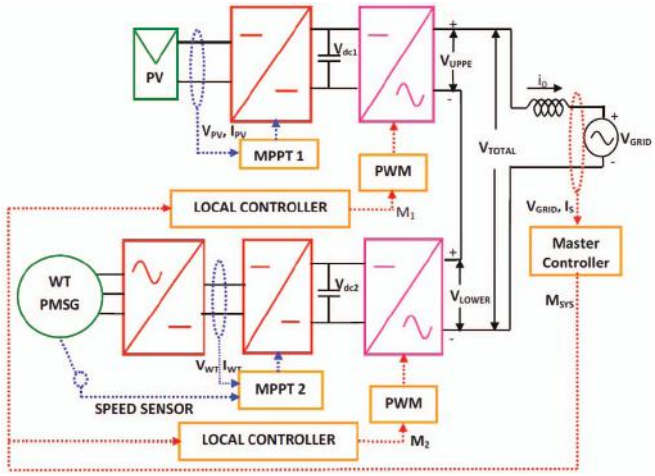

Fig. 7. Proposed Control System for cascaded MLI.

$$[p_1 + p_2] - p_{loss} = V_{rms} I_{rms} = V_{rms} \frac{i_{pk}}{\sqrt{2}} \tag{14}$$

Where p_1 and p_2 are the power delivered from PV module and WT. Assuming losses are small so that ploss is approximately zero than (13) can be rewritten as,

$$\sqrt{2} \frac{1}{V_{rms}} [p_1 + p_2] = i_{pk} \tag{15}$$

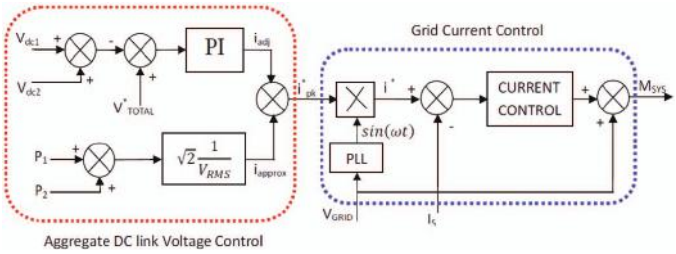

Fig. 8. Master Controller.

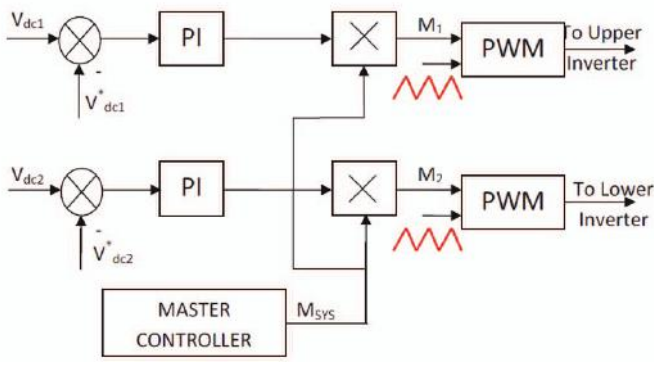

Fig. 9. Local Controllers.

It then follows that the quantity, i_{approx}, in Fig. 8 is approximately equal to the required peak output current for energy balance. However, because losses are uncertain and non zero, an adjustment term, i_{adj}, is necessary. This adjustment

term is generated by comparing the aggregate dc-link voltage to a fixed set point, V^*_{TOTAL} and feeding the error to a PI controller. The aggregate dc voltage command value, V^*_{TOTAL} must be chosen sufficiently higher than the peak grid ac voltage. The sum of i_{approx} and iadj then form the peak output current command i^*_{pk}.

The second stage of the master controller is designed to synchronize to the grid and regulate the output current. As shown in Fig. 1 and Fig 7, the measured grid voltage is utilized by a phase-locked-loop (PLL) to generate a sinusoidal reference, $sin\,(\omega t)$, which is in phase with the grid voltage. Here it is assumed that operation at unity power factor is desired. The PLL is conventional, as outlined in [27]-[32], for the proposed application. A sinusoidal current reference is created by multiplying the peak current command with sin (t). Lastly, a conventional current controller can be used to generate the system level modulation signal, M_{SYS}, which then goes to the both the local controllers.

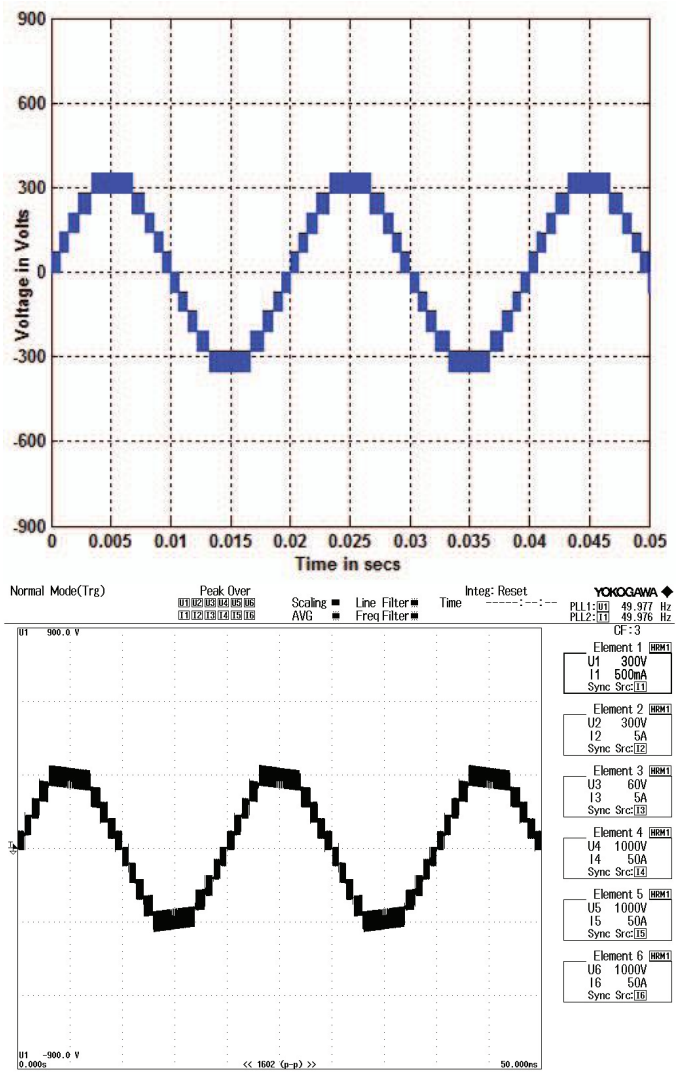

Fig. 10. Inverter output voltage with modulation index of 0.95 (a) Simulation (b) Experiment.

B. Local Controller

The collection of two local controllers is shown in Fig. 9. The primary purpose of each controller is to regulate the dc-link voltage of its respective sub-inverter. As shown, each dc-link voltage is compared to a fixed dc reference, V^*_{dc1} and V^*_{dc2}. This voltage reference is related to the aggregate dc-link command by

$$V^*_{dc1} = \frac{V^*_{TOTAL}}{5}, V^*_{dc2} = 4 * \left(\frac{V^*_{TOTAL}}{5}\right) \qquad (16)$$

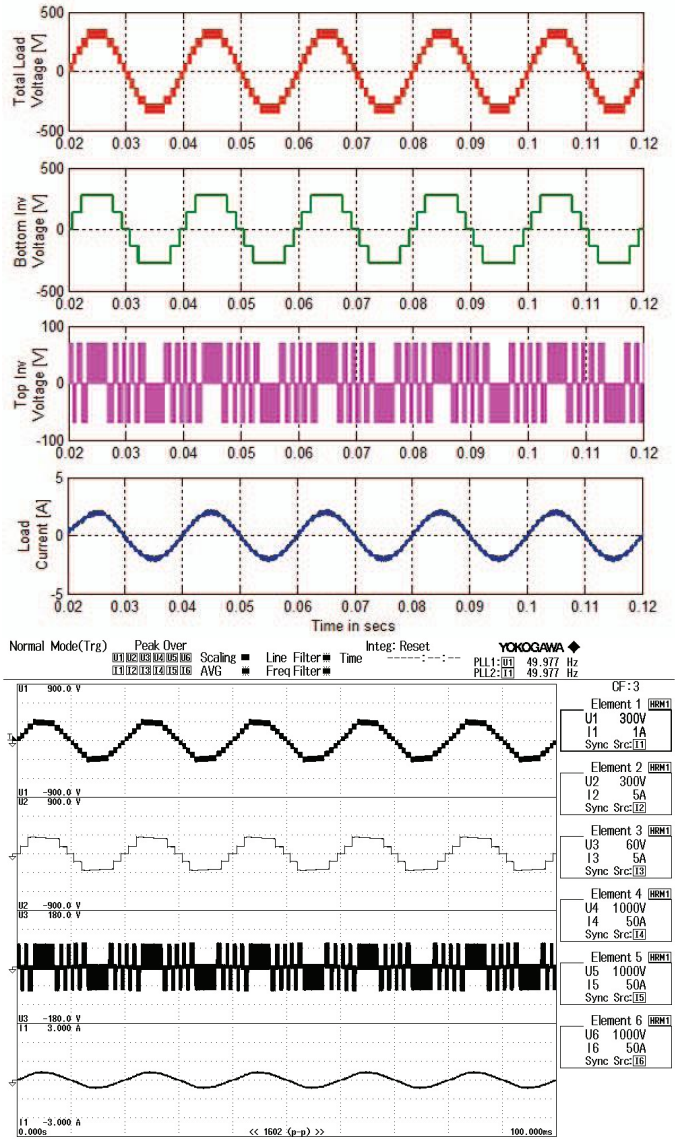

Fig. 11. Total, Upper and Lower Inverter voltage along with load current of the proposed CHBMLI (a) Simulation (b) Experiment.

The output of the 1st and 2nd PI controller is then multiplied by the master modulation signal,M_{SYS}, to create the local modulation signal M_1 and M_2. Ultimately, the local modulation signals and interleaved carriers are used to generate PWM signals which control both H-bridge inverters. As the modulation signal, M_1, is decreased in amplitude, the output power of the 1st sub-inverter decreases and the upper dc link

capacitor charges up. Alternatively, the upper dc link capacitor is discharged more heavily as the modulation depth of M_1 increases.

V. Results and Discussions

The simulation of the proposed eleven-level grid-connected hybrid PV and WECS is simulated using MATLAB/SIMULINK before it is implemented experimentally as a prototype. The PWM switching logics for the proposed CHBMLI is developed by using the expressions (4), (7) - (10). The Upper inverter is switched at high frequency (i.e. 10 KHz) and the lower inverter is switched at a frequency close to fundamental (i.e. 50 Hz). The Upper inverter dc bus voltage is set to 70 volts and the lower inverter dc bus voltage is set to four times the upper inverter voltage (i.e. 280 volts). So the net dc link voltage is set to 350 volts ($> \sqrt{2}V_{grid}$); in this case V_{grid} is 230V).

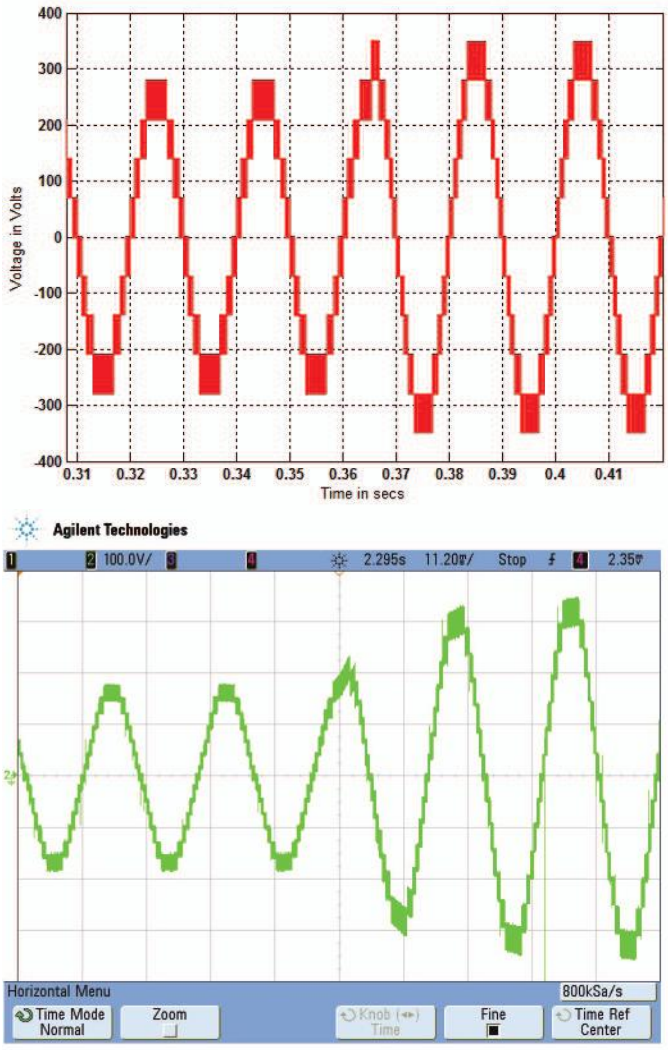

Fig. 12. Dynamic response of Inverter voltage for sudden change in grid voltage (a) Simulation (b)Experiment.

The total dc bus voltage should be always greater than $\sqrt{2}$ to inject current into the grid, else current will be injected from the grid into the inverter. Therefore, it is recommended to operate the inverter between modulation indices of 0.8 to 1. Fig. 10 shows the simulated and hardware waveforms obtained from the prototype of the proposed 11-level inverter with modulation index of 0.95. Fig 11 simulation and experimental results of the inverter output voltage supplied to the load along with the Upper and lower inverter voltage.

In order to study the dynamic behavior of the proposed inverter, grid voltage is disturbed from 180 V RMS to 230 V RMS at 0.35 secs in simulation. It can be noticed from fig 12 that due to sudden change in the grid voltage, the proposed inverter is capable of tracking the grid voltage automatically, by adjusting its amplitude modulation index. Fig 12 (b) shows the waveform obtained from the developed prototype for sudden perturbation in the grid voltage.

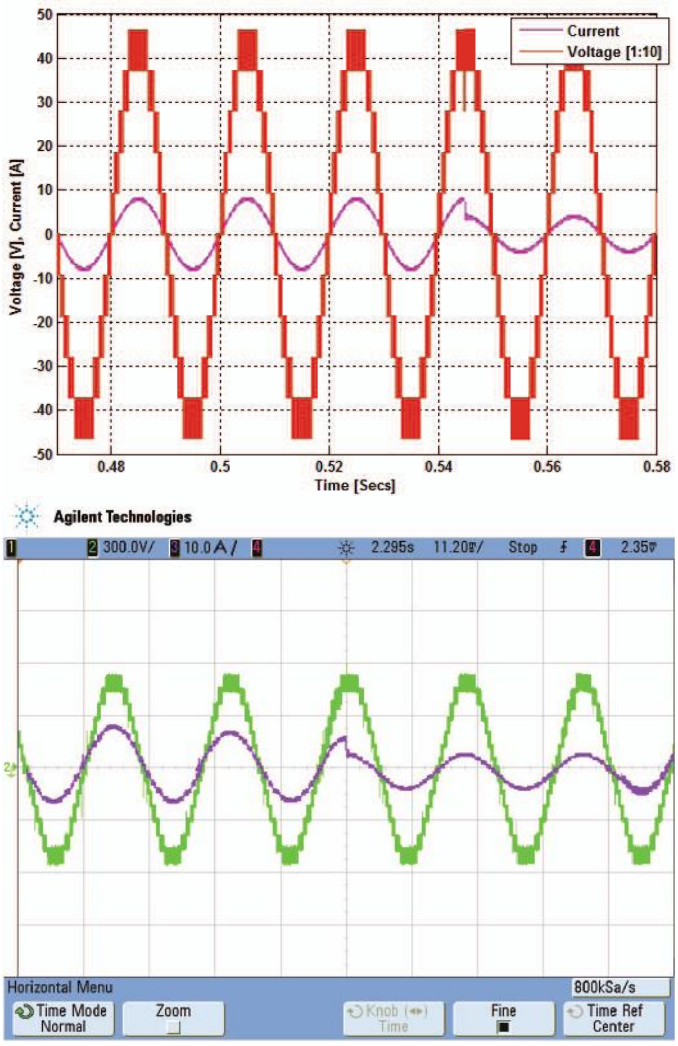

Fig. 13. Dynamic response of current supplied by the inverter to grid for sudden change in solar irradiance (a) Simulation (b) Experiment.

Fig 13 shows the simulated and experimental waveforms obtained due to sudden drop in the irradiance level from 1000 W/m^2 to 800 W/m^2. It can be observed in fig 13, that the current supplied by the PV source drops down due to fall in irradiance.

Fig 14 shows the voltage and current injected into the grid when both PV module and wind turbine operated at their rated

environmental conditions (i.e. 1000 W/m^2 and 10 m/s). When the environmental condition changes, the RMS magnitude of current injected into the grid also changes in proportional. From fig 14, the amount of RMS current injected into the grid is 9.35 amperes and the total power injected into the grid is about 2 KW.

VI. Conclusions

This paper has presented a novel single phase eleven inverter with reduced switching devices and isolated DC sources with sliding mode based MPPT algorithm. Simulations are carried out in MATLAB/Simulink and prototype model was also developed for 2.4 KW. Entire control system is developed by using FPGA board. The results obtained from simulation and experiment match perfectly with each other. This proposed CHBMLI system offers the advantage of reduced number of isolated DC sources and switching devices when compared to the conventional cascaded H bridge inverter. In addition, high frequency switching devices are operated at low voltage and low frequency devices are operated at high voltage, due to which the efficieny of the entire system is high compared to conventional CHB inverters. The eleven-level inverter can perform the functions of regulating the dc bus voltages of Upper and lower inverter and convert PV power and WT power into ac power with sinusoidal current in phase with the grid voltage. The experimental results shows that the developed photovoltaic power generation system, WECS and the eleven-level inverter achieves the expected performance.

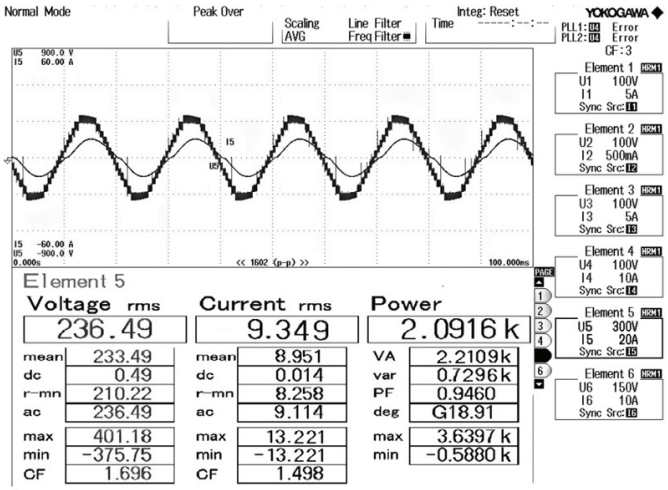

Fig. 14. Power injected into the Grid for Irradiance of 1000 W/m^2 and 10 m/s of wind speed.

References

[1] M. Carrasco, L. G. Franquelo, J. T. Bialasiewcz, E. Galvan, R. C. P. Guisado, M. A. M. Prats, J. I. Leon, and N. Moreno-Alfonso,*"Power-electronic systems for the grid integration of renewable energy sources: A survey," IEEE Trans. Ind. Appl., vol. 53, no. 4, pp. 10021016, Jul./Aug. 2006.*

[2] Nami, A., Zare, F., Ghosh, A., and Blaabjerg, F,*"A hybrid cascade converter topology with series-connected symmetrical and asymmetrical diode-clamped H-bridge cells," IEEE Trans. Power Electronics, vol. 26, no. 1, pp. 51-65,2011.*

[3] Tolbert, L. M., and Peng, F. Z.,*"Multilevel converters as a utility interface for renewable energy systems," IEEE Power Engineering Society Summer Meeting, vol. 2, pp. 1271-1274,2000.*

[4] Calais, Martina, Vassilios G. Agelidis, and Mike Meinhardt, *"Multilevel converters for single-phase grid connected photovoltaic systems: an overview" Solar Energy Vol. 66 no.5 1999, 325-335.*

[5] Merahi, Farid, El Madjid Berkouk, and Saad Mekhilef,*"New management structure of active and reactive power of a large wind farm based on multilevel converter." Renewable Energy Vol. 68 2014, 814-828.*

[6] Merahi, F., and Berkouk, E. M. *"Back-to-back five-level converters for wind energy conversion system with DC-bus imbalance minimization"* Renewable Energy, Vol. 60,2013 137-149.

[7] Guerrero-Perez, J., De Jodar, E., Gmez-Lzaro, E., and Molina-Garcia, A *"Behavioral modeling of grid-connected photovoltaic inverters: Development and assessment."* Renewable Energy, Vol. 68, 2014, 686-696.

[8] Sastry, J., Bakas, P., Kim, H., Wang, L., and Marinopoulos, A *"Evaluation of cascaded H-bridge inverter for utility-scale photovoltaic systems."* Renewable Energy, Vol.69,2014, 208-218

[9] Rahim, N. A., Selvaraj, J., and Krismadinata, C.*"Five-level inverter with dual reference modulation technique for grid-connected PV system."* Renewable Energy, Vol.35, No.3, 2010, 712-720.

[10] Calais, M., Agelidis, V. G., and Dymond, M. S.*"A cascaded inverter for transformer less single-phase grid-connected photovoltaic systems."* Renewable Energy, Vol. 22, No.1,2001, 255-262.

[11] Testa, A., De Caro, S., La Torre, R., and Scimone, T. *"A probabilistic approach to size step-up transformers for grid connected PV plants."* Renewable Energy, Vol.48, 2012, 42-51.

[12] Fekete, K., Klaic, Z., and Majdandzic, L. *"Expansion of the residential photovoltaic systems and its harmonic impact on the distribution grid."* Renewable Energy, Vol.43, 2012, 140-148.

[13] Alexander, S. A., and Thathan, M. *"Reduction of Voltage Harmonics in Solar Photovoltaic fed Inverter of Single Phase Stand Alone Power System."* Journal of Solar Energy Engineering, Vol. 136, No.4,2014, 044501.

[14] Zheng, H., Li, S., Challoo, R., and Proano, J. *2014 "Shading and bypass diode impacts to energy extraction of PV arrays under different converter configurations."* Renewable Energy, Vol.68,2014, 58-66.

[15] Kaliamoorthy, M., Rajasekaran, V., and Gerald Christopher Raj, I. *"Single-phase fifteen-level grid-connected inverter for photovoltaic system with evolutionary programming based MPPT algorithm."* Solar Energy, Vol. 105, 2014, 314-329.

[16] Sridhar, R., Jayasankar, K. C., Dash, S. S., and Avasthy, V. *"A Single Stage Photovoltaic Inverter With Common Power Factor Control and Maximum Power Point Tracking Circuit."* Journal of Solar Energy Engineering, Vol. 136, No.2, 2014, 021020.

[17] Muoz, F. J., Jimnez, G., Fuentes, M., and Aguilar, J. D. E*"Power Gain and Daily Improvement Factor in Stand-Alone Photovoltaic Systems With Maximum Power Point Tracking Charge Regulators.Case of Study: South of Spain."* Journal of Solar Energy Engineering, Vol. 135, No.4,2013, 041011.

[18] Averbukh, M., Ben-Galim, Y., and Uhananov, A. *2013 "Development of a Quick Dynamic Response Maximum Power Point Tracking Algorithm for Off-Grid System With Adaptive Switching (OnOff) Control of dc/dc Converter."* Journal of Solar Energy Engineering, Vol. 135,No.2,2013,021003.

[19] Adinolfi, G., Femia, N., Petrone, G., Spagnuolo, G., and Vitelli, M.*"Design of dc/dc Converters for DMPPT PV Applications Based on the Concept of Energetic Efficiency."* Journal of Solar Energy Engineering, Vol. 132, No.2, 2010, 021005.

[20] Azevedo, G. M. S., Cavalcanti, M. C., Oliveira, K. C., Neves, F. A. S., and Lins, Z. D. *"Comparative evaluation of maximum power point tracking methods for photovoltaic systems."* Journal of Solar Energy Engineering, Vol. 131, No.3,2009,031006.

[21] Radziemska, E., and Klugmann, E*"Photovoltaic maximum power point varying with illumination and temperature."* Journal of solar energy engineering,Vol.128, No.1,2006, 34-39

[22] Venkataramanan, G., Milkovska, B., Gerez, V., and Nehrir, H. *"Variable speed operation of permanent magnet alternator wind turbines using a single switch power converter."* Journal of solar energy engineering, Vol.118, No.4,1996, 235-238.

[23] Esram, T., and Chapman, P. L. *"Comparison of photovoltaic array maximum power point tracking techniques."* IEEE transactions on energy conversion ec, Vol.22, No.2,2007, 439

[24] D. Shmilovitz*"On the control of photovoltaic maximum power point tracker via output parameters."* IEE Trans. Power Appl.,Vol.152, No.2,2005, 239248.

[25] Jain, S., and Agarwal, V. *"A new algorithm for rapid tracking of approximate maximum power point in photovoltaic systems."* Power Electronics Letters, IEEE, Vol.2, No.1,2004,16-19.
[26] Sera, D., Teodorescu, R., Hantschel, J., and Knoll, M. *"Optimized maximum power point tracker for fast changing environmental conditions."* IEEE International Symposium on Industrial Electronics, 2008, 2401-2407.
[27] Blaabjerg, F., Teodorescu, R., Liserre, M., and Timbus, A. V. *"Overview of control and grid synchronization for distributed power generation systems."* Industrial Electronics, IEEE Transactions on, Vol.53, No.5,2006, 1398-1409
[28] Anani, N., Al-Kharji, O., Ponnapalli, P., Al-Araji, S., and Al-Qutayri, M.*"Synchronization of A single-phase photovoltaic generator with the low-voltage utility grid."* Journal of Solar Energy Engineering, Vol.134, No.1,2012, 011007.
[29] Naderi, P.*"Distributed Generation, Using Battery/Photovoltaic System: Modeling and Simulation With Relative Controller Design."* Journal of Solar Energy Engineering, Vol.135, No.2,2013, 024506
[30] Munoz, F. J., Torres, M., Munoz, J. V., and Fuentes, M. *"Monitoring Array Output Current and Voltage in Stand Alone Photovoltaics Systems With Pulse Width Modulated Charge Regulators."* Journal of Solar Energy Engineering,Vol.135, No.2, 2013, 021008.
[31] Henze, G. P., and Dodier, R. H. *"Adaptive optimal control of a grid-independent photovoltaic system."* Journal of solar energy engineering, Vol.125, No.1, 2003, 34-42.
[32] Jayashri, R., and Devi, R. K. *"Facts controllers for grid connected wind energy conversion systems."* Journal of Solar Energy Engineering, Vol.131, No.1,2009, 011008
[33] Kaliamoorthy, M., S. Himavathi, and A. Muthuramalingam. *"DSP based implementation of high performance flux estimators for speed sensorless induction motor drives using TMS320F2812."* Power Electronics, 2006. IICPE 2006. India International Conference on. IEEE, 2006.
[34] Kaliamoorthy, M., V. Rajasekaran, I. Gerald Christopher Raj and L. Hubert Tony Raj."Experimental Validation of Cascaded Single Phase H Bridge Inverter with Simplified Switching Algorithm." Journal of Power Electronics, vol.14, no.3, pp.507-518 , 2014

M.Kaliamoorthy graduation is in Electrical and Electronics Engineering from K.S.Rangasamy College of Engineering and Technology, Tiruchengodu, Tamilnadu, India in 1999 and his Post-Graduation is in the specilization of Electrical Drives and Control from Pondicherry Engineering College, Puducherry, India in 2006. He received a Gold medal for being the topper during his PG studies from Pondicherry University for his outstanding performance. His main area of interest includes multilevel inverters, Power Electronics for renewable energy sources and Induction Motor drives. He has nearly a decade of experience in teaching both under graduates and Post graduates. At present, he is working as an Associate Professor at PSNA College of Engineering and Technology, Dindigul, Tamilnadu, India. For further details, please do visit www.kaliasgoldmedal.yolasite.com.

V.Rajasekaran completed his B.E., and M.E (Power Systems) from Thiyagaraja College of Engineering, Madurai in 1993 and 1999 respectively. Later, he obtained his Ph.D degree from Madurai Kamarajar University, Madurai in 2008. He is a certified auditor of Energy auditing and serves as a consultant for various industries. At present, he is Professor and Head of electrical and Electronics Engineering at PSNA College of Engineering and Technology, Madurai, Tamilnadu, India.

G.Praveenraj completed his B.E., from PSNA College of Engineering,Dindigul in 2011. At present he is doing his masters in power electronics and drives in the same institute. His research interest includes Renewable energy and multilevel inverters.